

# Suppressed Superconductivity of the Surface Conduction Layer in Bi<sub>2</sub>Sr<sub>2</sub>CaCu<sub>2</sub>O<sub>8+x</sub> Single Crystals Probed by *c*-Axis Tunneling Measurements

Nam Kim, Yong Joo Doh, Hyun-Sik Chang, and Hu-Jong Lee

*Department of Physics, Pohang University of Science and Technology*

*Pohang 790-784, Republic of Korea*

## Abstract

We fabricated small-size stacks on the surface of Bi<sub>2</sub>Sr<sub>2</sub>CaCu<sub>2</sub>O<sub>8+x</sub> (BSCCO-2212) single crystals with the bulk transition temperature  $T_c \simeq 90$  K, each containing a few intrinsic Josephson junctions. Below a critical temperature  $T'_c$  ( $\ll T_c$ ), we have observed a weakened Josephson coupling between the CuO<sub>2</sub> superconducting double layer at the crystal surface and the adjacent one located deeper inside a stack. The quasiparticle branch in the  $IV$  data of the weakened Josephson junction (WJJ) fits well to the tunneling characteristics of a  $d$ -wave superconductor<sup>(')</sup>/insulator/ $d$ -wave superconductor (D'ID) junction. Also, the tunneling resistance in the range  $T'_c < T < T_c$  agrees well with the tunneling in a normal metal/insulator/ $d$ -wave superconductor (NID) junction. In spite of the suppressed superconductivity at the surface layer the symmetry of the order parameter appears to remain unaffected.

## I. INTRODUCTION

Bi<sub>2</sub>Sr<sub>2</sub>CaCu<sub>2</sub>O<sub>8+x</sub> (BSCCO-2212) single crystals of small lateral dimensions have been confirmed to exhibit intrinsic Josephson tunneling properties along the  $c$  axis<sup>1-3</sup> due to their layered structure, where the neighboring superconducting CuO<sub>2</sub> double layers (3 Å thick)

separated by 12-Å-thick non-superconducting Bi-O and Sr-O layers<sup>1</sup> form a series stack of superconductor-insulator-superconductor tunnel junctions. Since the  $c$ -axis coherence length for BSCCO-2212 single crystals<sup>4</sup>  $\xi_c$  is only  $\sim 1$  Å, the coupling between CuO<sub>2</sub> double layers is almost negligible except between the nearest-neighbor ones so that tunneling properties of each intrinsic Josephson junction can be well distinguished. One can fabricate stacks with junction area as small as a few hundreds of  $\mu\text{m}^2$  or less on the surface of BSCCO-2212 single crystals, each stack containing only a few intrinsic Josephson junctions. From its current-voltage ( $IV$ ) characteristics one can infer the superconducting characteristics of each conduction layer. It has been proposed, for instance, that the superconducting order may develop in the Bi-O layer due to the proximity location to the CuO<sub>2</sub> double layer.<sup>2</sup> Also the quasiparticle tunneling characteristics seen in the  $IV$  curves were analyzed in terms of the  $d$ -wave superconductivity in the conduction layers.<sup>3,5</sup>

Recently there has been interest in the properties of the surface layer of high- $T_c$  superconductor (HTSC) single crystals.<sup>6,7</sup> The interest stems from the realization that the useful tools to examine the superconducting properties of the HTSC materials, such as the vacuum tunneling spectroscopy and the photoemission spectroscopy, effectively probe only the surface properties of the crystals. On the other hand, in the case of transport measurements for HTSC single crystals, one needs to deposit metallic contact electrodes on the crystal surface. Aside from the possible degrading effect on the surface layer such as the contamination or the deviation from the optimal stoichiometry due to oxygen loss, deposition of a normal metal on the crystal surface changes the boundary condition of the surface CuO<sub>2</sub> double layer along with the corresponding changes in its physical properties. Until recently, however, few studies have been done for the effects of normal-metal deposition on the properties of the surface conduction layer.

In this study, we show that  $c$ -axis tunneling measurements in stacks of a few intrinsic tunnel junctions fabricated on the surface of HTSC single crystals can provide valuable information on the superconducting characteristics of the surface conduction layer in contact

with the normal electrode. From the  $IV$  curves of the stacks we identified the development of a Josephson junction right on the surface with much weakened Josephson coupling, which was directly related to the suppressed superconductivity in the surface conduction layer. The tunneling  $IV$  curve and the  $c$ -axis resistive transition  $R(T)$  of the stacks supported the existence of predominant  $d_{x^2-y^2}$  symmetry in the  $\text{CuO}_2$  double layers including the one at the crystal surface. The temperature dependence of both the critical current ( $I'_c$ ) of this weakened “surface junction” and that ( $I_c$ ) of the “inner junctions” embedded under the surface junction did not follow the Ambegaokar-Baratoff relation.<sup>8</sup>  $I'_c(T)$  showed a tail near the critical temperature  $T'_c$  of the weakened Josephson junction (WJJ). We propose that the anomalous features as well as the suppression of the superconductivity in the surface layer resulted from the change in the surface boundary conditions rather than material degradation of the surface layer itself, which is believed to occur in an unprotected surface of a HTSC material.

## II. EXPERIMENT

BSCCO-2212 single crystals were grown by solid-state-reaction method. Powders of  $\text{Bi}_2\text{O}_3$ ,  $\text{SrCO}_3$ ,  $\text{CaCO}_3$ , and  $\text{CuO}$  were mixed, thoroughly ground, and heat treated in an alumina crucible. The mixing molar ratio of Bi:Sr:Ca:Cu was 2.3:2:1:2. During the crystal growth process, a constant oxygen gas was provided and a temperature gradient of about 5 °C/cm was set up across the diameter of the crucible to enhance the growth rate. Platelets of as-grown single crystal with typical size of  $0.7 \times 0.2 \times 0.03 \text{ mm}^3$  were glued on MgO substrates using negative photoresist (OMR-83) and were cleaved with Scotch-brand tape until optically smooth surfaces were obtained. Upon cleaving a BSCCO-2212 single crystal a 500-Å-thick layer of Au was thermally deposited on the top of the crystal to protect the surface from contamination during further fabrication process as well as to obtain a clean interface between the normal electrodes and the BSCCO-2212 single crystal. Stacks of size  $25 \times 35 \times 0.015 \text{ } \mu\text{m}^3$  were then patterned using the conventional photolithography with pos-

itive photoresist (Microposit 1400-23) and the Ar-ion-etching technique. Further details of the sample fabrication are described elsewhere.<sup>9</sup>

Temperature dependence of the  $c$ -axis resistance  $R(T)$  of a stack was measured by conventional lock-in technique and the  $IV$  data were taken using a dc method for two different stacks #E and #F, which were fabricated simultaneously on the same crystal surface. Contact configurations are shown in Fig. 1(a). All measurements were done in a three-terminal configuration using low pass filters connected to each measurement electrode. The bias current was fed to the stack #E (#F) through the electrodes E and A (F and A) while the voltage was taken between the electrodes E and F (F and B). Three-terminal configuration was adopted to probe the surface junction by intentionally including the potential drop across the surface layer.

### III. RESULTS AND DISCUSSION

In a three-terminal configuration, the  $c$ -axis resistance of a stack consists of the tunneling resistance of the stacked intrinsic tunnel junctions ( $R_{stack}$ ), both the one at the surface and the one(s) under the surface, and the contact resistance ( $R_c$ ) between the Au electrode and the BSCCO-2212 single crystal including the resistance of the Au electrode itself. We present all of our data below with  $R_c$  ( $\simeq 1.7 \Omega$ ) subtracted, assuming that  $R_c$  is temperature independent and ohmic. The assumption is justified by the fact that the contact resistance  $R_c$  is represented by a linear portion below the critical current  $I'_c$  in the raw  $IV$  data (not shown) taken at 4.2 K and by the negligible temperature dependence of  $R_c$  compared with  $R_{stack}$ . The normal-state tunneling resistivity of the stack #E at  $\sim 100$  K was  $\rho_c = 35 \Omega\text{cm}$ .

The  $IV$  data of the stack #F taken at 4.2 K [Fig. 2(a)] show a superconducting branch and the usual multiple quasiparticle branches. Although not shown, the stack #E exhibited very similar feature. The multiple branches develop since each intrinsic Josephson junction in a stack with a slightly different critical current from one another switches separately to the resistive state with increasing the bias current beyond  $I_c$ . From the number of the branches

one can easily estimate the number of the junctions (or the number of the  $\text{CuO}_2$  double layers) contained in a stack, which turns out to be 10 (11) for the stack #F. Each junction shows almost vertical current variation just before switching to the resistive state. Exceeding the critical current the  $IV$  characteristics of each junction exhibit a characteristic voltage jump  $V_c$ . The value of  $V_c$  upon exceeding  $I_c$  is  $\sim 23$  meV and, as observed previously,<sup>1</sup> it decreases progressively as the number of junctions involved increases, which may be related to the nonequilibrium effect.<sup>10</sup> The critical current  $I_c$  in our samples turned out to be larger by a factor than that reported previously by others,<sup>2,3,5,10</sup> which may have resulted in a larger nonequilibrium effect. All the multiple branches beyond  $I_c$  exhibit large hysteresis, which is a characteristic of an underdamped junction.

In Fig. 2(a), we notice that the critical current of one junction is much smaller than those of the rest of the junctions, *i.e.*,  $I'_c$  ( $\sim 0.14I_c$ ), at which one of the 10 Josephson junctions switches to the resistive state. This feature of the WJJ appears only below  $T'_c$  [ $=35$  K  $\approx 0.39T_c$ ,  $T_c$  the critical temperature of the bulk BSCCO-2212 single crystal; see Fig. 3(a)]. For the samples we tested in this study, the value of  $T'_c$  varied from sample to sample in the range  $20 \text{ K} \lesssim T'_c \lesssim 40 \text{ K}$ . The possible reason for this variation of  $T'_c$  will be discussed below. The WJJ also shows hysteresis corresponding to the McCumber parameter<sup>11</sup>  $\beta_c$  of  $\sim 5$ , which is about 100 times smaller than that of the inner Josephson junctions [Fig. 2(b)]. Recently, in the  $IV$  curve of a stack fabricated on a BSCCO-2212 crystal in the same way as used in this study, Kim *et al.* observed zero-current-crossing voltage steps<sup>12</sup> in the resistive state of the WJJ at voltages of  $n\hbar\nu/2e$  ( $n$  is an integer and  $\nu$  is the frequency of the rf excitation) with  $\sim 90$  GHz rf excitation. It is a strong evidence that the junction of the weakened coupling forms a single Josephson junction.

In Fig. 2(b) we compare the behavior of the quasiparticle branch of the WJJ with the results of numerical calculation. The  $IV$  curve was calculated using the expression

$$I(V) = \frac{1}{eR_n} \int_{-\infty}^{\infty} N(E)N(E+eV) [f(E) - f(E+eV)] dE \quad (1)$$

where  $R_n$  is the normal-state tunneling resistance and  $f(E)$  the Fermi distribution func-

tion. As for the quasiparticle density of states  $N(E)$  we used the expression for the  $d_{x^2-y^2}$  symmetry<sup>3,5,13</sup> as

$$N(E) = Re \left[ \frac{1}{2\pi} \int_0^{2\pi} \frac{E}{\sqrt{E^2 - [\Delta_0 \cos(2\theta)]^2}} d\theta \right] \quad (2)$$

by modeling the surface Josephson junction as a  $d$ -wave superconductor(')/insulator/ $d$ -wave superconductor (D'ID, D' denotes an electrode with suppressed  $d$ -wave superconductivity) junction with the parameter values of  $\Delta_0^D=30$  meV,  $\Delta_0^{D'}=(T'_c/T_c)\Delta_0^D=0.39\Delta_0^D$ , and  $R_n=2.3$   $\Omega$ , where  $\Delta_0^D$  and  $\Delta_0^{D'}$  are  $\Delta_0$  for D and D', respectively [see Fig. 1(b)]. The value of  $\Delta_0^D$  turns out to be close to the one of the previous reports.<sup>3,5</sup> The fairly good fit with reasonable parameter values again strongly suggests that the junction of the weakened coupling bears the Josephson nature with both CuO<sub>2</sub> layers of predominant  $d_{x^2-y^2}$  symmetry. With the much smaller  $I'_c$  and the lower  $T'_c$  than the other intrinsic Josephson junctions, the superconducting order parameter of one of the 11 CuO<sub>2</sub> double layers must be significantly suppressed with the resultant weakened interlayer coupling across the corresponding junction(s). Since the CuO<sub>2</sub> double layer of the suppressed superconductivity affects the characteristics of only one junction instead of two the layer must be the topmost one located closest to the stack surface. The location of the WJJ on the surface has also been ascertained by measurements using *in situ* thickness control of a stack by Doh and Lee.<sup>9</sup> The authors observed that the tunneling characteristics of the WJJ appeared prior to the appearance of any other multiple branches in the  $IV$  characteristics.

As to the cause of the order parameter suppression, we pay attention to the fact that the CuO<sub>2</sub> double layer at the crystal surface is in contact with the normal Au electrode, while the inner CuO<sub>2</sub> double layers are Josephson coupled to the neighboring ones. Deutcher and Müller<sup>6</sup> predicted suppression of the pair potential of a HTSC with a short  $c$ -axis coherence length  $\xi_c$  when in contact with a non-superconducting layer perpendicular to it.<sup>14</sup> This proximity effect of the normal metal on the superconductivity of HTSC are not well understood to date. Although not directly applicable to HTSC systems, the McMillan model<sup>15</sup> for conventional superconductors predicts that the superconducting transition temperature  $T_{NS}$  of

the S electrode in a normal-metal/superconductor (NS) junction depends on the thickness of each metal and the electron scattering strength at the interface between N and S. The model predicts that the thinner the S layer is in comparison with the N layer, the less stable the superconductivity becomes in the S layer. Since the  $\text{CuO}_2$  double layer is extremely thinner than the Au electrode, we may assume that the pair potential in the surface  $\text{CuO}_2$  layer was significantly suppressed.

Fig. 3(a) shows the temperature dependence of the  $c$ -axis tunneling resistance  $R(T)$  for the stacks #E and #F with the measurement configuration as illustrated in Fig. 1(a). Although the stacks #E and #F were fabricated simultaneously on the same crystal surface, the resistance of the stack #F, just above  $T_c$  ( $\simeq 90$  K), is about a factor of two larger than that of the stack #E, presumably because the voltage for the stack #F was across more junctions [including the ones in the larger base as illustrated in Fig. 1(a)] than for the stack #E. Nonetheless, the  $R(T)$  data below  $T_c$  for both stacks #E and #F merge to a single curve, showing a single peak at  $T'_c$  ( $\simeq 35$  K) and an ensuing abrupt superconducting transition. This suggests again that the resistive curve in the range  $T'_c < T < T_c$  is a surface effect, the same one as adopted for the analysis of the  $IV$  curves. In the intermediate temperature range  $T'_c < T < T_c$ , the inner  $\text{CuO}_2$  double layers below the surface conducting layer are superconducting while the surface  $\text{CuO}_2$  double layer remains normal due to its suppressed superconductivity [Fig. 1(b)]. Thus, as far as the low-bias resistive state is concerned, each stack in this temperature range behaves like a single NID junction (N denotes a normal electrode). Due to the thermally assisted nature of the quasiparticle tunneling from N to D, the tunneling resistance of the surface junction increases with decreasing temperature until the weakly coupled Josephson junction forms at  $T'_c$ . Assuming  $N(E+eV)=1$  in Eq. (1) along with the BCS-type temperature dependence of the gap  $\Delta_0$  in Eq. (2), one can calculate the temperature dependence of the tunneling resistance  $R$  for a NID junction from the relation  $R = (dI/dV)^{-1}|_{V=0}$  using the same value of the gap energy ( $\Delta_0^D=30$  meV) as used for the  $IV$ -curve calculations in Fig. 2(b). We used the normal-state tunneling resistance  $R_n$  ( $=1.55$   $\Omega$ ) as the fitting parameter, which is reasonably close to the value  $R_n=2.3$   $\Omega$  used in the

$IV$ -curve calculations [Fig. 2(b)]. Below  $T_c$ , the calculated  $R(T)$  curve (dotted line) shows almost the same curvature and fits rather well to the measured  $R(T)$  data of both stacks. Also, illustrated in Fig. 3(b) is the gradual change of the  $IV$  characteristics of the WJJ with temperature. One clearly notices that a D'ID-like behavior of the surface junction with hysteresis gradually transforms into a monotonous NID-like behavior with a finite subgap states in D as the temperature approaches  $T'_c$  from below [refer to Fig. 1(b)].

Since the weakened Josephson coupling is considered to be a phenomenon related to the proximity coupling between the superconducting surface  $\text{CuO}_2$  double layer and the normal-metallic electrode, it should be absent for a four-terminal configuration (where the  $\text{CuO}_2$  layers at the surface under the current and voltage contacts are separated) or in a stack with heat-treated contact electrodes. In the latter case no sharp boundary between the normal electrode and the  $\text{CuO}_2$  double layer can be defined due to the thermal interdiffusion of the composition materials. Yurgens *et al.*<sup>16</sup> also reported, without interpretation, similar secondary resistance peak in  $R(T)$  like ours far below  $T_c$  for a three-terminal measurement configuration, while no such feature was observed by the authors in a four-terminal configuration. No feature of the WJJ was reported from other experiments,<sup>2,10</sup> where either four-terminal configuration or heat-treated electrodes were used. The typical feature of the WJJ was observed in all the samples we examined, when the data were taken in a three-terminal configuration, although  $T'_c$  and  $I'_c$  may differ from sample to sample. Currently we have no clear explanation for the relatively large variation of  $T'_c$  and  $I'_c$  for different samples, while the values of  $T_c$  were reproducible. As mentioned above, however, since the  $T_{NS}$  of S in a NS junction is sensitive to the scattering barrier or the contact resistance of the junction, we suppose that the lack of reproducibility of  $T'_c$  and  $I'_c$  may be due to the sample-to-sample difference in  $R_c$ . The coupling between two adjacent Bi-O layers is known to be weakest in the BSCCO-2212 crystal. Thus, upon cleaving, a Bi-O layer is most likely to be surfaced. However, the influence of the existence of this layer on the suppression of the order parameter in the surface  $\text{CuO}_2$  double layer is currently unclear and is a subject of further study.



We have also obtained the temperature dependence of the critical current  $I'_c(T)$  and the return current  $I'_r(T)$  of the WJJ (Fig. 4) from the measured  $IV$  characteristics. In the low temperature region the values of  $I'_c$  have rather high fluctuations, which may be attributed to the multi-valued critical current induced by fluxon motions in the long junction limit<sup>17</sup> [junction width > Josephson penetration depth ( $\lambda_J \sim 1 \mu\text{m}$ ) for BSCCO-2212]. The  $I'_c(T)$  curves for both stacks #E and #F strongly deviate from the Ambegaokar-Baratoff expression and exhibit a long tail in the range  $\frac{1}{2}T'_c \lesssim T \lesssim T'_c$ . On the other hand, the critical current  $I_c(T)$  of the inner Josephson junctions does not show the tail structure (see the inset of Fig. 4). Curiously enough,  $I_c(T)$  appears to follow the temperature dependence of the BCS superconducting gap. The tail structure of  $I'_c(T)$  cannot be explained by the present S'IS- or D'ID-type single junction model<sup>11,18</sup> (S' denotes a superconducting electrode with suppressed  $s$ -wave superconductivity). This anomalous temperature dependence of the WJJ in comparison with the inner Josephson junctions may provide the clues to the origin of the suppressed superconductivity. Studies on the temperature dependence of the critical current have been done, both theoretically and experimentally, for NSIS-type proximity junctions consisting of conventional superconductors.<sup>19,20</sup> In an experimental work<sup>20</sup> with conventional superconductors Camerlingo *et al.* observed a small tail in the critical current near the transition temperature, although theoretical calculations<sup>19</sup> did not predict the tail structure.

In conclusion, in stacks of intrinsic Josephson junctions formed on the surface of BSCCO-2212 single crystals, we have observed a WJJ presumably between the surface superconducting layer and the adjacent inner superconducting layer at temperatures below  $T'_c=35$  K, significantly lower than the  $T_c$  of the bulk BSCCO-2212 single crystals. The quasiparticle branch in the  $IV$  data of the surface Josephson junction fits well to the tunneling behavior of the assumed D'ID-type junction. We could also explain the increase in its tunneling resistance with decreasing temperature below  $T_c$ , assuming the surface junction as a NID junction. The proximity location of the surface conduction layer to the normal electrode suppresses the superconductivity in the surface layer. Nonetheless, apparently it does not

alter the symmetry of the suppressed superconductivity, the predominant  $d_{x^2-y^2}$  nature remains intact. Despite the qualitative agreements between some experimental data and the single junction model, we still need more comprehensive theoretical treatment for the superconducting characteristics existing at the surface of high- $T_c$  superconductors. Although the suppression of the superconducting order in the surface  $\text{CuO}_2$  layer is certainly an unfavorable phenomenon for any device application it may still be positively utilized to study the microscopic properties of the inner  $\text{CuO}_2$  layer such as the quasiparticle density of states using the  $c$ -axis NID tunnel-junction configuration. It can also be exploited to study the order parameter symmetry of HTSC materials by forming a conventional-superconductor/high- $T_c$ -superconductor  $c$ -axis hybrid junction, since the symmetry of the surface layer does not change from that of the bulk.

#### IV. ACKNOWLEDGMENTS

This work was supported by the Korea Science and Engineering Foundation under Contract No. 1NK9700501, BSRI administrated by the Ministry of Education under Contract No. 1RB9811401, and the Ministry of Defense through MARC under Contract No. 1MC9801301.

## REFERENCES

- <sup>1</sup> R. Kleiner, F. Steinmeyer, G. Kunkel, and P. Müller, Phys. Rev. Lett. **68**, 2394(1992); R. Kleiner and P. Müller, Phys. Rev. B **49**, 1327 (1994).
- <sup>2</sup> A. Yurgens, D. Winkler, N. V. Zavaritsky, and T. Claeson, Phys. Rev. B **53**, R8887 (1996).
- <sup>3</sup> K. Schlenga, R. Kleiner, G. Hechtfischer, M. Mößle, S. Schmitt, Paul Müller, Ch. Helm, Ch. Preis, F. Forsthofer, J. Keller, H. L. Johnson, M. Veith, and E. Steinbeiß, Phys. Rev. B **57**, 1 (1998).
- <sup>4</sup> T. T. M. Palstra, B. Bätlogg, L. F. Schneemayer, R. B. van Dover, and J. V. Waszczak, Phys. Rev. B **38**, 5102 (1988); J. H. Kang, R. T. Kampwirth, and K. E. Gray, Appl. Phys. Lett. **52**, 2080 (1988).
- <sup>5</sup> M. Itoh, S. Karimoto, K. Namekawa, and M. Suzuki, Phys. Rev. B **55**, R12001 (1997).
- <sup>6</sup> G. Deutscher and K. A. Müller, Phys. Rev. Lett. **59**, 1745 (1987).
- <sup>7</sup> T. Giamarchi, M. T. Béal-Monod, and Oriol T. Valls, Phys. Rev. B **41**, 11033 (1990); S. H. Liu, and R. A. Klemm, Phys. Rev. B **52**, 9657 (1995); Stephen W. Pierson, and Oriol T. Valls, Phys. Rev. B **45**, 2458 (1992); R. S. Gonnelli, D. Puttero, G. A. Ummarino, V. A. Stepanov, and F. Licci, Phys. Rev. B **51**, 12782 (1995).
- <sup>8</sup> V. Ambegaokar and A. Baratoff, Phys. Rev. Lett. **10**, 486 (1963); **11**, 104(E) (1963).
- <sup>9</sup> Yong Joo Doh and Hu-Jong Lee, *Proceedings of the 8th Conference on Materials and Applications of Superconductivity, Yong-Pyung, Korea, 1998*.
- <sup>10</sup> K. Tanabe, Y. Hidaka, S. Karimoto, and M. Suzuki, Phys. Rev. B **53**, 9348 (1996).
- <sup>11</sup> A. Barone, *Physics and Applications of the Josephson Effect* (John Wiley & Sons, Inc. 1982).
- <sup>12</sup> Jinhee Kim, Kyu-Tae Kim, Se Il Park, Yong Joo Doh, Nam Kim, and Hu-Jong Lee (unpublished).

- <sup>13</sup> H. Won and K. Maki, Phys. Rev. B **49**, 1397 (1994).
- <sup>14</sup> In the theory, however,  $d$ -wave symmetry was not assumed in the HTSCs. The relevance to the HTSCs was introduced only in terms of extremely short  $c$ -axis coherence length.
- <sup>15</sup> W. L. McMillan, Phys. Rev. **175**, 537 (1968).
- <sup>16</sup> A. Yurgens, D. Winkler, N. V. Zavaritsky, and T. Claeson, Proc. SPIE **2697**, 433 (1996).
- <sup>17</sup> N. Mros, V. M. Krasnov, A. Yurgens, D. Winkler, and T. Claeson, Phys. Rev. B **57**, R8135 (1998).
- <sup>18</sup> Yukio Tanaka and Satoshi Kashiwaya, Phys. Rev. B **56**, 892 (1997).
- <sup>19</sup> V. Z. Kresin, in *Josephson Effect: Achievements and Trends*, edited by A. Barone (World Scientific, Singapore, 1985), p.198.
- <sup>20</sup> C. Camerlingo, R. Monaco, B. Ruggiero, M. Russo, and G. Testa, Phys. Rev. B **51**, 6493 (1995).

## FIGURES

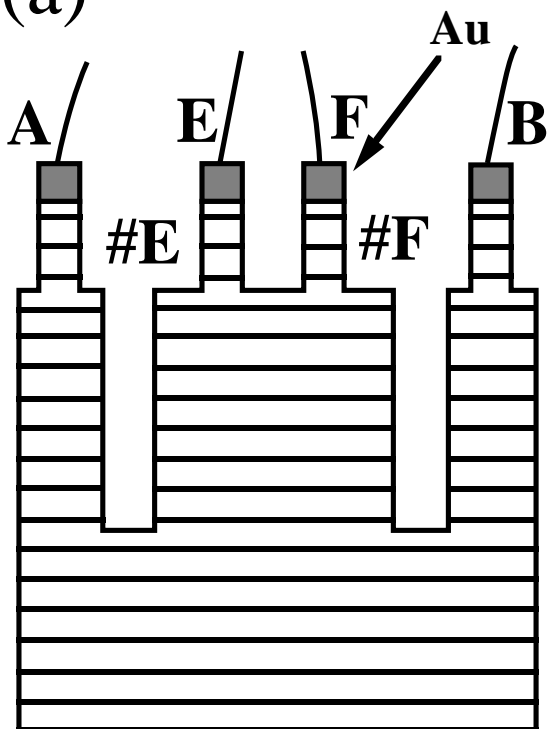
FIG. 1. (a) Schematic diagram of the stacks fabricated on a BSCCO-2212 single crystal. The size of the stacks #E and #F is  $25 \times 35 \times 0.015 \text{ } \mu\text{m}^3$ . Measurement configuration of the current and the voltage is as follows:  $I(\text{E} \rightarrow \text{A})$ ,  $V(\text{E} \rightarrow \text{F})$  for the stack #E;  $I(\text{F} \rightarrow \text{A})$ ,  $V(\text{F} \rightarrow \text{B})$  for the stack #F. (b) Schematic structure of a stack near the surface in the temperature ranges  $T < T'_c$  and  $T'_c < T < T_c$ , respectively. As discussed in the text the Au electrode and the surface  $\text{CuO}_2$  double layer form an ohmic contact. The insulating barrier (I) is believed to form between neighboring Bi-O layers.

FIG. 2.  $IV$  curves for the stack #F measured at 4.2 K are plotted with the contact resistance subtracted. (a) Multiple quasiparticle branches with the critical current of the surface junction ( $I'_c$ ) and that of the inner junction ( $I_c$ ). (b) The  $IV$  curve of the surface junction (solid curve) showing a hysteresis. The dotted curve shows the calculated  $IV$  curve for a D'ID junction using Eqs. (1) and (2) with  $\Delta_0^D = 30 \text{ meV}$ ,  $\Delta_0^{D'} = 11.6 \text{ meV}$ , and  $R_n = 2.3 \text{ } \Omega$ .

FIG. 3. (a) The  $R(T)$  curve of the stacks #E (circle) and #F (triangle) for a bias current  $I_b = 0.5 \text{ } \mu\text{A}$  with the contact resistance  $1.72 \text{ } \Omega$  subtracted. Dotted curve exhibits the calculated fit with  $\Delta_0^D = 30 \text{ meV}$  and  $R_n = 1.55 \text{ } \Omega$ . (b) The  $IV$  curves of the WJJ for the stack #E at various temperatures. The curves are displaced horizontally for clarity. As the temperature approaches  $T'_c$  from below the critical current as well as the hysteresis gradually disappear.

FIG. 4. Temperature dependence of critical current of the surface Josephson junction  $I'_c(T)$  of the stacks #E (solid circle) and #F (open circle), and the return current  $I'_r$  (dotted line) of the stack #E. Inset: temperature dependence of the critical current of an inner junction  $I_c(T)$  of the stack #E (solid circle). The BCS gap relation (solid line) and the AB relation (dotted line) are plotted together.

(a)



(b)

